ADVANCED PHOTONICS RESEARCH Open Access
www.adpr-journal.com

Unequilibrated Charge Carrier Mobility in Organic Semiconductors Measured Using Injection Metal–Insulator–Semiconductor Charge Extraction by Linearly Increasing Voltage

Mile Gao, Paul L. Burn, Gytis Juška, and Almantas Pivrikas**

The charge carrier mobility in tris(4-carbazoyl-9-ylphenyl)amine (TCTA), a host and hole transport material typically used in organic light-emitting diodes (OLEDs), is measured using charge carrier electrical injection metal–insulator–semiconductor charge extraction by linearly increasing voltage (i-MIS-CELIV). By employing the injection current i-MIS-CELIV method, charge transport at time scales shorter than the transit times typically observed in standard MIS-CELIV is measured. The i-MIS-CELIV technique enables the experimental measurement of unequilibrated and pretrapped charge carriers. Through a comparison of injection and extraction current transients obtained from i-MIS-CELIV and MIS-CELIV, it is concluded that hole trapping is negligible in evaporated neat films of TCTA within the time-scales relevant to the operational conditions of optoelectronic devices, such as OLEDs. Furthermore, photocarrier generation in conjunction with i-MIS-CELIV (photo-i-MIS-CELIV) to quantify the properties of charge injection from the electrode to the semiconductor of the MIS devices is utilized. Based on the photo-i-MIS-CELIV measurements, it is observed that the contact resistance does not limit the injection current at the TCTA/molybdenum oxide/silver interface. Therefore, when TCTA is employed as the hole transport/electron-blocking layer in OLEDs, it does not significantly reduce the injection current and remains compatible with the high injection current densities required for efficient OLED operation.

1. Introduction

The performance of organic light-emitting diodes (OLED) is dependent on the injection current and hence on the transport of holes and electrons.[1,2] It is therefore critical to be able to measure the mobility of each charge carrier type. Metal–insulator–semiconductor charge extraction by linearly increasing voltage (MIS-CELIV) has been used in the past to measure the extraction current transients associated with charge carriers that have been selectively injected and accumulated at an organic semiconductor/insulator interface by a constant offset voltage.[3–6] The time required to accumulate the charge at that interface during application of the offset voltage also allows charges to fill localized trap states in the semiconductor layer.[5] Hence, the nature of charge transport measured using MIS-CELIV can in principle be different to that of operational devices, especially devices operating in the frequency or time domain. Charge carrier trapping within a hole or electron transporting layer will reduce the charge carrier mobility and injection current, which in the case of organic semiconductor devices such as OLEDs, can negatively impact the device performance.[7]

Current methods to quantify the charge carrier trapping-related parameters in disordered materials are mainly based on complex data fitting from steady-state current–voltage characteristics. MIS-CELIV can be used to selectively determine hole and electron mobilities, and it is also possible to gain some insight into whether charges are trapped in the semiconductor layer from an estimation of the amount of extracted charge and

M. Gao, P. L. Burn
Centre for Organic Photonics & Electronics
The School of Chemistry and Molecular Biosciences
The University of Queensland
Queensland 4072, Australia
E-mail: p.burn2@uq.edu.au

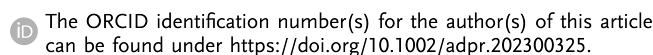
The ORCID identification number(s) for the author(s) of this article can be found under https://doi.org/10.1002/adpr.202300325.

© 2024 The Author(s). Advanced Photonics Research published by Wiley-VCH GmbH. This is an open access article under the terms of the Creative Commons Attribution License, which permits use, distribution and reproduction in any medium, provided the original work is properly cited.

DOI: 10.1002/adpr.202300325

G. Juška
Institute of Chemical Physics
Vilnius University
Saulėtekio al. 3, 10257 Vilnius, Lithuania

A. Pivrikas
Physics Department
Murdoch University
Perth, Western Australia 6150, Australia
E-mail: a.pivrikas@murdoch.edu.au

the full-width-at-half-maximum (FWHM) of the extraction transient.[8] A narrow transient FWHM indicates less charge trapping, while materials with strongly dispersive charge transport with a significant number of charges trapped in the organic semiconductor layer will have an extraction current peak that is typically less well-defined due to the distribution of charge carrier transit times.[9] It is important to note that the amount of charge trapped is sensitive to the charge injection time used in the MIS-CELIV experiment, which can be significantly longer than the charge carrier transit time or the lifetime of a charge in an operational device such as an OLED.[10] A benefit of using MIS-CELIV for charge transport studies is that the measurement has less dependency on the resistance of injecting contact. The reduced dependence on the resistance of the injecting contact arises from the long duration of the applied offset voltage (much longer than the transit time), which is generally sufficient to achieve the situation whereby the semiconductor/insulator interface is fully charged for subsequent charge extraction.[11] However, in rare cases, the contact resistance of the injecting contact can be too high, and the time required to fully charge the semiconductor insulator interface can set a practical limit on application of the MIS-CELIV technique.

We have therefore developed an approach to address the potential issues of MIS-CELIV mobility measurements with regards to charge trapping and injection, with the aim to determine charge transport on timescales of relevance to OLEDs. Instead of measuring charge extraction, as for the standard MIS-CELIV experiment, we measure injection current transients in MIS-CELIV device geometries. An advantage of this approach is that it allows measurement of the mobility of injected charge carriers, and hence mirrors charge injection and transport in an OLED. A side benefit of this method is that it allows for a direct estimation of the thicknesses of both the semiconductor and insulator layers in the MIS-CELIV device architecture directly from the current transient. A further outcome of the charge injection-MIS-CELIV (i-MIS-CELIV) measurement is that it enables quantification of the dielectric permittivity of the semiconductor simultaneously with charge carrier mobility. This is an important issue not just for OLEDs but for other semiconducting materials such as perovskites, which contain large densities of mobile ions or dipoles.[12]

In the second part of the study, we used photoexcitation to generate charge carriers[13] to isolate the potential effects of contact resistance, which can limit the injection current and cause the charging times of the semiconductor/insulator interface to be much longer than the extraction transit time in the standard MIS-CELIV experiment, both of which might lead to erroneous interpretation of the current transients.[10] To demonstrate these new techniques, we studied evaporated films of tris(4-carbazoyl-9-ylphenyl)amine (TCTA), which is a host and hole transport material typically used in OLEDs. The charge transport properties of TCTA have been measured using different techniques and hence are a good exemplar to test the new techniques against.

2. Results and Discussion

Figure 1 shows the operating principles of the i-MIS-CELIV measurement: first, the triangular voltage pulse, as shown in Figure 1a, is applied to the MIS structure, with the current transient response (response signal) recorded using an oscilloscope. The details of how the devices were fabricated and measured are

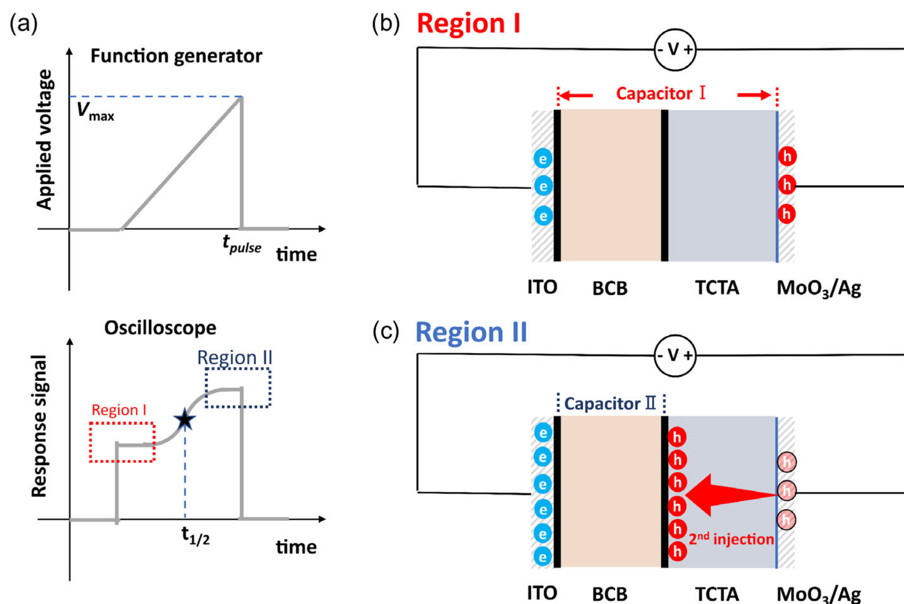

Figure 1. Schematic illustrating the i-MIS-CELIV technique. An applied triangular voltage pulse is shown in a) together with the recorded current transient response. The sample forms a MIS geometry composed of two capacitors connected in series represented by region I (BCB + TCTA capacitances connected in series) as shown in b), while region II is the capacitance of the BCB insulator only, as shown in c). Note, the amount of charge in capacitor II is larger than capacitor I, hence the response signal is larger in region II. The transit time can be estimated from the time it takes for the current to rise to the maximum value, region II.

© 2024 The Author(s). Advanced Photonics Research published by Wiley-VCH GmbH

26999293, 2024, 9, Downloaded from https://onlinelibrary.wiley.com/doi/10.1002/adpr.202300325 by Vilnius University, Wiley Online Library on [05/02/2025]. See the Terms and Conditions (https://onlinelibrary.wiley.com/terms-and-conditions) on Wiley Online Library for rules of use; OA articles are governed by the applicable Creative Commons License

described in the Experimental Section. While the results in the Figures are exemplar traces, at least six devices of each type were tested to ensure the reliability and reproducibility of the method. The transient response is divided into two regions; the first region (marked as region I) has both the insulating Cyclotene 3022-35 (BCB) and semiconductor TCTA layers acting as a combined capacitive layer, with the second (region II) only being determined by the capacitance of the BCB.

During the applied triangular voltage ramp, the displacement current is flat in region I due to the charging of capacitor I (semiconductor and insulator connected in series, as shown in Figure 1b). As the triangular voltage increases more charge is injected into the semiconductor, and in addition, the charge carrier transport accelerates due to an increase in the electric field, which results in a rising transient response till the injected charge reaches and charges capacitor II. At this point the current plateaus in region II (insulator capacitance II, shown Figure 1c). The time taken to reach the point at which the current value is halfway between the current plateaus of regions I and II is defined as $t_{1/2}$, which we use to explain the observed differences in the current transients.

Recent advances in the i-CELIV technique have addressed the influence of recombination rate and ohmic contacts by introducing correction factors.[10,14] However, it is important to note that the i-CELIV correction factors are not universal, and not directly applicable to i-MIS-CELIV. For example, the impact of charge trapping remains a variable and, if present, can impact the mobility calculations by orders of magnitude. This is important as most organic semiconductor films are disordered, which means that there are often charge traps leading to dispersive transport.

As stated earlier, we have applied i-MIS-CELIV to quantify the hole mobility in TCTA as an exemplar of the method. To record the variation of the charge carrier transit through the semiconductor, we varied the maximum voltage of the triangular pulse (V_{max}). **Figure 2** shows the i-MIS-CELIV charge injection transients, with flat regions I and II (explained in Figure 1) clearly visible. It should be noted that the i-MIS-CELIV transients do not result in a current peak, as is the case in classical CELIV or MIS-CELIV.[15] The polarity of the applied triangular voltage was chosen to cause hole injection into the semiconductor layer, as TCTA is not ambipolar. When the applied voltage V_{max} was increased, $t_{1/2}$ was observed to decrease for the same pulse duration time. This is expected because an increased electric field increases the charge drift velocity leading to a shorter transit time. The slightly increasing current in region II of the transient at $V_{max} = 25$ V is caused by leakage of the current through the BCB insulator under the large applied electric field.

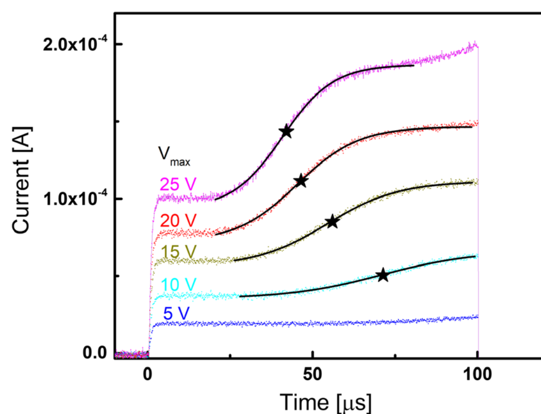

Figure 2. Experimental i-MIS-CELIV current transients (dots) for various V_{max} of the triangular voltage pulse whilst keeping the same pulse duration, and the numerical data fits (solid black lines). Note, $t_{1/2}$ (marked by black stars) decreases with increasing V_{max} as expected due to the increased charge drift velocity at higher applied electric fields.

Numerical simulations were used to fit the experimental current transients, which allowed estimation of the charge carrier mobility values. The charge carrier (hole) mobility was estimated from numerical fits of the current transients (shown in Figure 2 as solid lines) to be $(3.0 \pm 1.0) \times 10^{-6}$ cm^2 V^{-1} s^{-1}. The variance in the mobility determined from the experimental data fits when using different V_{max} was small (<20% of the absolute value). The $t_{1/2}$ was observed to vary with V_{max} as expected, due to an increase in drift velocity at higher electric fields. This degree of variance is a common feature of all CELIV techniques, which arises from the use of the triangular voltage pulse changing the electric field. Hence, when using any of the CELIV techniques, the effect of the change in the electric field needs to be considered during the analysis of the data. A previous study of MIS-CELIV measurements showed that the mobility can be overestimated depending on the contact resistance, such that at small transient voltages ($A * t_1 < 0.5$) an overestimation of the mobility of several orders of magnitude can be introduced. The overestimation required a correction factor to be included during the analysis.[10]

We next compared the charge carrier mobility values measured for TCTA from i-MIS-CELIV with standard MIS-CELIV experiments.[16] The i-MIS-CELIV transients arise from the injection of holes, whereas in the MIS-CELIV experiment, the transient is due to the extraction of the accumulated holes from a charge reservoir at the semiconductor/insulator interface. We note that comparative measurements were undertaken on separate devices to avoid any effect of differential charge trapping affecting the results. The hole mobility value of TCTA was reported to be 7.5×10^{-5} cm^2 V^{-1} s^{-1} from the MIS-CELIV transient in which a $V_{max} = 15$ V was used, although it should be noted that mobilities determined using MIS-CELIV have a similar sensitivity to V_{max} (25% increase as a function of V_{max}).[6] A comparison of the hole mobility values determined from the i-MIS-CELIV and MIS-CELIV measurements shows that the former was close to an order of magnitude lower than the latter. The i-MIS-CELIV mobility was $(3.0 \pm 1.0) \times 10^{-6}$ cm^2 V^{-1} s^{-1}.

The difference in mobility values between the two measurement techniques could arise from a variety of reasons including a high resistance between the injecting contact and semiconducting layer (noting that i-MIS-CELIV is an injection technique), the nature of the charge population within the density-of-states, or the different filling of trap states.[17] In fact, it is critical when comparing mobilities from different device architectures to note the geometry of the measurement as these can lead to the semiconducting chromophores having different alignments relative to the direction of the field. Furthermore, significantly different fields arising from the effective channel lengths and applied voltage (static or dynamic) can affect the density-of-states occupation and trap filling and hence the measured charge mobility.[17]

 © 2024 The Author(s). Advanced Photonics Research published by Wiley-VCH GmbH

26999293, 2024, 9, Downloaded from https://onlinelibrary.wiley.com/doi/10.1002/adpr.202300325 by Vilnius University, Wiley Online Library on [05/02/2025]. See the Terms and Conditions (https://onlinelibrary.wiley.com/terms-and-conditions) on Wiley Online Library for rules of use; OA articles are governed by the applicable Creative Commons License

26999293, 2024, 9, Downloaded from https://onlinelibrary.wiley.com/doi/10.1002/adpr.202300325 by Vilnius University, Wiley Online Library on [05/02/2025]. See the Terms and Conditions (https://onlinelibrary.wiley.com/terms-and-conditions) on Wiley Online Library for rules of use; OA articles are governed by the applicable Creative Commons License

To identify whether deep trap states or the contact resistance was the origin of the mobility difference between the techniques, we applied two sequential triangular voltage pulses, as shown in **Figure 3**a. The second pulse followed the first pulse without a delay time. In the absence of trapped charge created by the first pulse, the transient response to the second pulse would be expected to be like the first. In addition, if the second current transient is similar to the first then this indicates that essentially all the charges have escaped from the film before injection starts during the second pulse.

It can be seen in Figure 3b that the difference between the current transients arising from the first and second voltage ramps is small, being essentially the same after 25 μs. This fact is consistent with the amount of deeply trapped charge being small (less than the space charge). The fact that there is a negligible amount of deeply trapped holes in TCTA explains why it is such a good hole transport material for efficient OLEDs. It should be noted that if there was a significantly large number of deeply trapped charges (much larger than the space charge density, which is defined as a product of dielectric permittivity and electric field), the Coulomb blockade effect would take place, resulting in orders of magnitude reduced charge carrier mobility as well as a change in the timescale of injection current transients. The numerical fit (solid lines) of the current transients shown in Figure 3b explains the difference in current between the first and second voltage pulses. Since there was no delay time between the applied injection voltage pulses, the second current transient response pulse was expected to be slightly slower due to the residual charge in the semiconductor, which reduces the effective applied electric field of the second triangular pulse. Hence it takes a longer time to reach the saturated displacement current in region II at the end of the second pulse.

Given that deep charge traps were not the reason for the nearly an order of magnitude lower hole mobility measured using i-MIS-CELIV (relative to MIS-CELIV), we next considered the effect of contact resistance on i-MIS-CELIV measurement. Note, that a four-probe approach cannot be applied to directly measure the contact resistance in a typical sandwich-type device such as an OLED. Since i-MIS-CELIV measures injection transients, there is a requirement that the contact resistance between the semiconductor and electrode should be much smaller than the resistance of the semiconductor. Otherwise, the injection current will be limited by the contact and hence the rise time will lead to an underestimation of the mobility values.[10] To resolve this potential issue, we photoexcited the semiconductor to generate free charges using the method shown in **Figure 4**a. The MIS-CELIV device was illuminated through the transparent indium tin oxide (ITO)/BCB layers, and the geometry and applied voltage polarity of the i-MIS-CELIV experiment were such that under the voltage ramp the holes formed by the photoexcitation were driven toward the semiconductor/insulator interface. Under these conditions, the insulator interface will be charged in a similar way to the case where electrically injected charges accumulate at the semiconductor/insulator interface in a standard MIS-CELIV experiment. Thus, using light to create mobile charges removes potential issues relating to a contact barrier or contact resistance between the TCTA film and the MoO_3/Ag contact in the photo-i-MIS-CELIV experiment.

The current transients from the i-MIS-CELIV and photo-i-MIS-CELIV measurements are shown in Figure 4b. The photo-i-MIS-CELIV transients demonstrate $t_{1/2}$ being at shorter timescales compared to the electrical injection case. The apparent decrease in $t_{1/2}$ for the photo-i-MIS-CELIV experiment arises from the fact that the charges are photogenerated in the volume of the semiconductor layer. Thus, for the photo-i-MIS-CELIV, the charges on average must travel only half the distance to the insulator-semiconductor interface. In contrast, the electrically injected charges in the i-MIS-CELIV experiment must move through the whole thickness of the semiconductor layer. Hence, the transient response and $t_{1/2}$ measured using dark i-MIS-CELIV is longer and the calculated mobility lower. That being said, the fact that the current transient responses in the light and the dark do not differ by orders of magnitude indicates that the resistance of the injecting contact does not significantly limit the injection current in the i-MIS-CELIV measurements on the TCTA films. A possible reason for the hole mobility measured in TCTA using the i-MIS-CELIV technique being lower than that measured using standard MIS-CELIV is the difference between the equilibrated charge transport within the partially filled density-of-states. However, it is important to note that

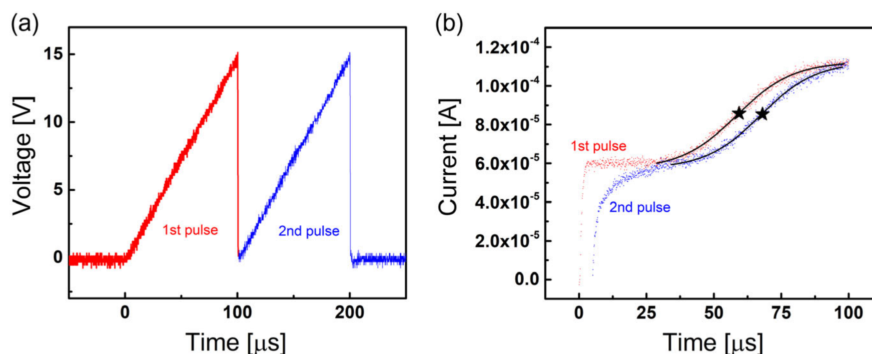

Figure 3. a) Two sequential applied triangular voltage pulses used in the i-MIS-CELIV experiment. b) Corresponding experimentally measured current transient responses (dots) and numerical data fits (solid lines). The similarity in the current transient responses between the first and the second pulses at time scale above 25 μs indicates that the amount of trapped charge is negligible compared to the space charge, hence, deep charge trapping states were not present in the studied devices.

© 2024 The Author(s). Advanced Photonics Research published by Wiley-VCH GmbH

26999293, 2024, 9, Downloaded from https://onlinelibrary.wiley.com/doi/10.1002/adpr.202300325 by Vilnius University, Wiley Online Library on [05/02/2025]. See the Terms and Conditions (https://onlinelibrary.wiley.com/terms-and-conditions) on Wiley Online Library for rules of use; OA articles are governed by the applicable Creative Commons License

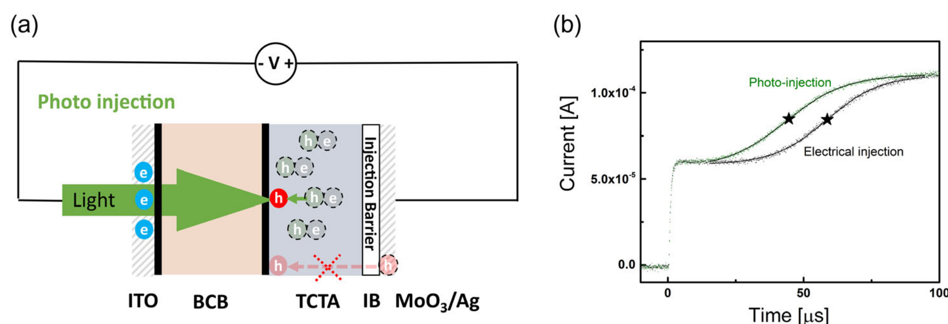

Figure 4. a) Photo-i-MIS-CELIV measurement setup ($\lambda_{exc} = 365$ nm). b) Experimentally measured current transient responses with and without photoexcitation (dots) and numerical data fits (solid lines). Note that the photoinjection transient is faster compared to the dark transient, as expected due to the effective transit length in the case of photoinjection. The lack of orders of magnitude difference in $t_{1/2}$ proves that the charge injection is not limited or blocked by the resistance of the injecting MoO_3/Ag contact.

despite the differences in $t_{1/2}$, the estimated hole mobility from the photo-i-MIS-CELIV and i-MIS-CELIV were observed to be the same, $(3.0 \pm 1.0) \times 10^{-6}$ cm^2 V^{-1} s^{-1}.

In conclusion, i-MIS-CELIV is introduced as a technique to study the charge transport dynamics and mobilities of injected charge, which is of direct relevance to electrically driven applications such as OLEDs. In contrast to a standard MIS-CELIV experiment, where the charge carrier mobility is measured from the extraction current transients, the i-MIS-CELIV technique allows the determination of the mobility from injected current transients. By using i-MIS-CELIV with two sequentially applied voltage pulses, we show that deep charge trapping does not occur in neat evaporated TCTA films. The photo-i-MIS-CELIV transients were similar to those from the i-MIS-CELIV measurements, indicating that the contact resistance in the exemplar devices was negligible and much lower than the resistance of the TCTA. Hence, i-MIS-CELIV overcomes the limitations of hole and electron-only devices, which generally suffer from trapping and contact resistance when used for charge transport measurements. The hole mobility measured from the MIS-CELIV extraction transients was observed to be higher than that from the i-MIS-CELIV experiments. In MIS-CELIV, the charge density is higher and all lower energy states, which would give rise to a low mobility if only they were filled, are filled and hence most of the extracted charge occurs through the higher energy states with higher mobilities. Thus, i-MIS-CELIV is more sensitive to shallow trap/density of states. The absence of deep charge trapping and low contact resistance in evaporated neat TCTA films are beneficial for high-performance OLEDs that use it as a hole transport/electron blocking layer. The presented i-MIS-CELIV and photo-i-MIS-CELIV methodology are applicable for a wide range of semiconductors and devices such as OLEDs, solar cells, photodetectors, or other electronic devices where electrical current impacts the device performance.

3. Experimental Section

The fabrication process of the ITO substrates has been previously reported.[16] The substrates were cleaned sequentially in aqueous Alconox, deionized water, acetone, and 2-propanol in an ultrasonic bath for 10 min and then dried using a nitrogen flow. BCB was diluted in a 1:4 volume ratio with mesitylene and a 60 nm-thick BCB layer was spin-coated at 5000 rpm for 30 s in a nitrogen-filled glovebox onto the cleaned substrate, before being annealed at 300 °C for 10 min. After being allowed to cool to room temperature, the substrates were transferred into an evaporation chamber. TCTA (rate ≈1 Å s^{-1}), MoO_3 (rate ≈ 0.2 Å s^{-1}), and Ag (rate ≈ 1 Å s^{-1}) were deposited sequentially by thermal vacuum evaporation using a Kurt J. Lesker SPECTROS evaporation system at a base pressure of 5×10^{-7} mbar. BCB was purchased from the Dow Chemical Company and TCTA was purchased from Luminescence Technology Corporation and used without further purification.

The i-MIS-CELIV measurement was carried out using a function generator (Tektronix 3052C), an oscilloscope (WaveRunner 6200 A; 2 GHz), and a voltage amplifier (Falco Systems WMA-320). For the i-MIS-CELIV and photo-i-MIS-CELIV measurements, the function generator with the positively rising triangular pulse was connected to the MoO_3/Ag side, while for MIS-CELIV, it was connected to the ITO side. For the photo-i-MIS-CELIV measurement, a UV lamp (UVP UVGL-55 from Analytik Jena) was used to photoexcite the organic semiconductor. All measurements were carried out at room temperature under vacuum.

The finite element method in 1D was employed to fit the time-dependent experimentally measured injection current transients using a set of normalized drift-diffusion equations reported in ref. [18]. The numerical model includes parameters for drift-diffusion and continuity equations, voltage and electric field, charge carrier density and mobility, the semiconductor/insulator thicknesses, and their permittivities. Dimensionless parameters were used in the simulation to minimize the computational resources required. Furthermore, the following equation was used to incorporate the measurement circuit (including contact resistance) in the model: RC $dU/dt = V_psu(t) - U(t) - I(t)R$, where the power supply unit generates a voltage waveform $Vpsu(t)$, which is applied to the RC circuit. The initial conditions for electron and hole densities in the device were set to zero based on the MIS-CELIV charge extraction experiments showing that the evaporated TCTA layer was not doped.[19] Furthermore, the parameters for charge carrier trapping and contact resistance were effectively zero based on the experimental observations and hence were not included as parameters in the model. Thus, the fitting parameters used were the following: semiconductor and insulator permittivity, RC, film thickness of semiconductor and insulator, applied voltage, and charge carrier mobility. In addition, the drift-diffusion equations for a MIS-CELIV device geometry were used.[20] Each parameter in drift-diffusion equations was normalized to a respective quantity following the method described in ref. [20]. For example, the charge carrier density was normalized to CU (where C is the device capacitance and U is the applied voltage), the transit time to the transit time of small charge (much smaller than the CU space charge, $t_{tr} = d^2/\mu/U$, where t_{tr} is the transit time, μ is the charge carrier mobility), and the voltage to the initial voltage applied in the transient simulation. The drift current, $I = e * n * mu * E * S$ (where e is the elementary charge, n is the charge carrier density, E is the electric field, and S is the surface area) was used as the charge injecting

 © 2024 The Author(s). Advanced Photonics Research published by Wiley-VCH GmbH

boundary condition for numerically solving the drift-diffusion equations. A boundary condition preventing charge outflow ($j = 0$) at the semiconductor/insulator interface was used. Boundary conditions for the triangular applied voltage were set on one electrode while the other electrode was grounded. The voltage was applied under forward bias conditions for the charge carrier injection through the electrode using the standard Dirichlet boundary conditions. Numerical fitting was performed on the experimental transient region starting at region I and ending at region II, as shown in Figure 1a.

Acknowledgements

The work was carried out at the Centre for Organic Photonics & Electronics at the University of Queensland. P.L.B. was an Australian Research Council (ARC) Laureate Fellow (FL160100067), and the work was supported by the fellowship. P.L.B. is currently a UQ Laureate Fellow. This work was performed in part at the Queensland node of the Australian National Fabrication Facility (ANFF-Q), a company established under the National Collaborative Research Infrastructure Strategy to provide nano- and microfabrication facilities for Australia's researchers. The authors acknowledge the facilities, and the scientific and technical assistance, of the Centre for Microscopy and Microanalysis, the University of Queensland, the Queensland node of Microscopy Australia. A.P. acknowledges support from ARC DP210102192.

Open access publishing facilitated by Murdoch University, as part of the Wiley - Murdoch University agreement via the Council of Australian University Librarians.

Conflict of Interest

The authors declare no conflict of interest.

Data Availability Statement

The data that support the findings of this study are available from the corresponding author upon reasonable request.

Keywords

charge extraction by linearly increasing voltage, charge transport, charge trapping, organic light-emitting diodes

Received: December 13, 2023
Revised: June 18, 2024
Published online: July 15, 2024

[1] J.-M. Kim, J.-J. Kim, *Org. Electron.* **2019**, *67*, 43.
[2] S. Xue, X. Qiu, S. Ying, Y. Lu, Y. Pan, Q. Sun, C. Gu, W. Yang, *Adv. Opt. Mater.* **2017**, *5*, 1700747.
[3] A. Armin, G. Juska, M. Ullah, M. Velusamy, P. L. Burn, P. Meredith, A. Pivrikas, *Adv. Energy Mater.* **2014**, *4*, 1300954.
[4] C. Katagiri, T. Yoshida, M. S. White, C. Yumusak, N. S. Sariciftci, *AIP Adv.* **2018**, *8*, 105001.
[5] W. J. Kim, Y. Nishikawa, T.-T. Bui, F. Goubard, Q.-D. Dao, A. Fujii, M. Ozaki, *Jpn. J. Appl. Phys.* **2020**, *59(SG)*, SGGG01.
[6] M. Gao, P. L. Burn, A. Pivrikas, *J. Appl. Phys.* **2019**, *126*, 035501.
[7] N. C. Giebink, B. W. Dändrade, M. S. Weaver, P. B. Mackenzie, J. J. Brown, M. E. Thompson, S. R. Forrest. *J. Appl. Phys.* **2008**, *103*, 044509.
[8] O. Semeniuk, G. Juska, J.-O. Oelerich, M. Wiemer, S. D. Baranovskii, A. Reznik, *Sci. Rep.* **2016**, *6*, 33359.
[9] R. Hanfland, M. A. Fischer, W. Brütting, U. Würfel, *Appl. Phys. Lett.* **2013**, *103*, 063904.
[10] O. J. Sandberg, M. Nyman, S. Dahlström, S. Sandén, B. Törngren, J.-H. Smått, R. Österbacka. *Appl. Phys. Lett.* **2017**, *110*, 153504.
[11] S. Züfle, S. Altazin, A. Hofmann, L. Jäger, M. T. Neukom, W. Brütting, B. Ruhstaller, *J. Appl. Phys.* **2017**, *122*, 115502.
[12] M. S. Alvar, P. W. M. Blom, G. A. H. Wetzelaer, *Nat. Commun.* **2020**, *11*, 4023.
[13] J. Peng, X. Chen, Y. Chen, O. J. Sandberg, R. Österbacka, Z. Liang, *Adv. Electron. Mater.* **2016**, *2*, 1500333.
[14] G. Juška, K. Genevicius, *Appl. Phys. Lett.* **2018**, *113*, 123301.
[15] G. Juška, N. Nekrašas, K. Genevicius, *J. Non-Cryst. Solids* **2012**, *358*, 748.
[16] M. Gao, T. Lee, P. L. Burn, A. E. Mark, A. Pivrikas, P. E. Shaw, *Adv. Funct. Mater.* **2020**, *30*, 1907942.
[17] V. I. Arkhipov, P. Heremans, E. V. Emelianova, G. J. Adriaenssens, H. Bässler, *J. Phys.: Condens. Matter* **2002**, *14*, 9899.
[18] S. Morab, M. Minakshi Sundaram, A. Pivrikas, *Nanomaterials* **2022**, *12*, 4414.
[19] O. J. Sandberg, M. Nyman, R. Österbacka, *Org. Electron.* **2014**, *15*, 3413.
[20] B. Philippa, C. Vijila, R. D. White, P. Sonar, P. L. Burn, P. Meredith, A. Pivrikas, *Org. Electron.* **2015**, *16*, 205.

© 2024 The Author(s). Advanced Photonics Research published by Wiley-VCH GmbH

26999293, 2024, 9, Downloaded from https://onlinelibrary.wiley.com/doi/10.1002/adpr.202300325 by Vilnius University, Wiley Online Library on [05/02/2025]. See the Terms and Conditions (https://onlinelibrary.wiley.com/terms-and-conditions) on Wiley Online Library for rules of use; OA articles are governed by the applicable Creative Commons License